Primary and Secondary Hopf Bifurcations in Stratified Taylor-Couette Flow

F. Caton, B. Janiaud,* and E. J. Hopfinger
LEGI, CNRS-UJF-INPG, B.P. 53 X, 38041 Grenoble Cedex 9, France
(Received 23 July 1998)

Experimental and theoretical results for the axially, stably stratified Taylor-Couette flow are presented. The primary instability is a direct Hopf bifurcation. It leads the system into an oscillatory state of confined internal waves, in good agreement with linear stability analysis. The secondary bifurcation, which leads the system to a pattern of drifting nonaxisymmetric vortices, is a subcritical Hopf bifurcation. This first experimental evidence of a global bifurcation is thought to be generic to dynamical systems with one destabilizing and one stabilizing control parameter. [S0031-9007(99)09248-0]

PACS numbers: 47.20.Ky, 47.54.+r, 47.55.Hd

The transition to chaos in extended nonlinear systems is still an open question [1–3]. The oscillatory nature of the primary bifurcation changes the scenario [4,5] and has not yet been fully explored. Such a primary Hopf bifurcation can be obtained by adding a stabilizing control parameter, allowing the existence of waves, to a dynamical system. Simply adding a stable, axial density stratification to the well-known Taylor-Couette flow [6], with only the inner cylinder rotating, allowed us to get such a rich dynamical system.

In this Letter we present new experimental and theoretical results of the stratified Taylor-Couette flow (STC) that describe its first bifurcations and flow regimes. A novel bifurcation diagram is found, explaining the discrepancies between previous experimental studies [7,8] and numerical simulations [9]. The diagram enlightens the interaction between two branches and gives evidence to an unusual saddle-node transition. Such a diagram has never been observed experimentally. Our results apply to other systems such as rotating Rayleigh-Bénard convection [5], binary fluid convection [10], and convection subjected to a magnetic field, where it has been suggested theoretically [11].

The apparatus, which is the same as in [7], consists of two coaxial cylinders of length $L = 573$ mm. Only the inner cylinder of radius $a = 40$ mm rotates, with the outer one $b = 52$ mm, being at rest. The radius ratio of the cylinders is $\eta = a/b = 0.769$ indicating a rather wide gap. The linear stratification is achieved with a salt solution. The control parameters are the rotation rate of the inner cylinder Ω (destabilizing parameter), and the Brunt-Vaïsälä frequency $N^2 = -(g/\rho_0)\partial\rho/\partial z > 0$ (stabilizing parameter) which represents the stratification; z is the vertical direction. The Schmidt number (ratio of kinematic viscosity over molecular diffusivity) is 730. In all experiments, the observations and measurements were performed for times much smaller than the typical mixing time in the regimes of interest ($\sim$5 h). In order to exhibit the structures in the different flow regimes, fluorescein dye, illuminated with a laser sheet cutting through the axis of the cylinders, is used. The temporal behavior of the flow was obtained by point measurements of the density fluctuations, using conductivity probes mounted flush with the outer cylinder. Two probes were fixed at the same height, at an azimuthal angle of $\pi/2$. The experimental setup and techniques are described in more detail elsewhere [12].

The numerical simulations of Hua *et al.* [9] show that the first bifurcation from a purely azimuthal Couette flow is a direct Hopf bifurcation, leading to a flow regime of "oscillatory convective modes." We present in Fig. 1(a) a dye visualization of this regime. The pattern has been captured for successive times in one vertical section of the gap. The initially vertical lines of dye are deformed by spatially periodic oscillations, their wavelength being

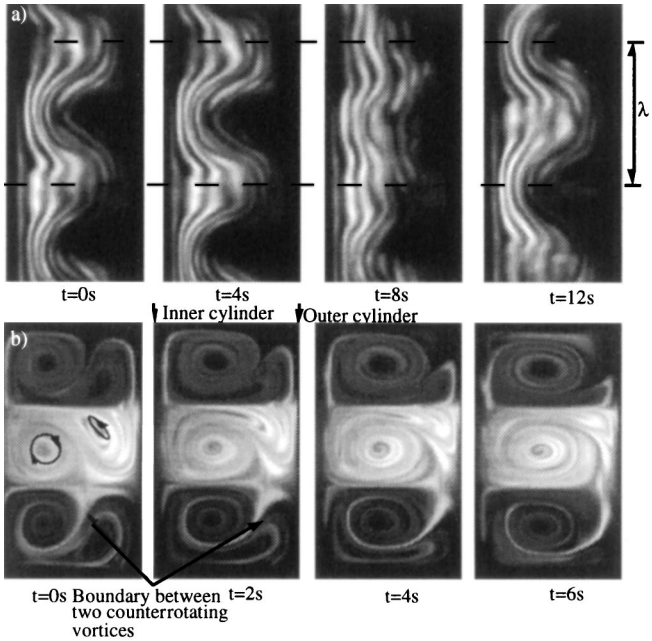

FIG. 1. Dye visualization of stratified Taylor-Couette flow $N = 0.97$ rad s^{-1}. (a) Standing waves regime $\Omega = 1.1\Omega_c$; (b) vortex regime $\Omega = 1.35\Omega_c$.

nearly equal to the gap width ($\lambda \simeq d$). In contrast to the homogeneous case, for which the first unstable regime is stationary (Taylor vortices) [6], the first unstable regime for the stratified case is time dependent. As underlined by previous studies [7,9], the reduction in the vertical wavelength as compared with the homogeneous case ($\lambda \simeq 2d$) is directly related to the inhibition of vertical motions by stratification. Time records of this pattern clearly show *oscillations*, the positions of the maxima and minima of oscillations being fixed. No overturning is observed in this regime, indicating *standing waves.*

The characteristics of the onset of instability were investigated by measurements of the temporal evolution of the density fluctuations. When the rotation rate of the inner cylinder is raised to the critical value Ω_c, the frequency of the waves appears in the power spectra, indicating a Hopf bifurcation. We first checked that this frequency depends only on the rotation rate and the stratification, and not on the experimental procedure. There is no hysteresis for the transition between purely azimuthal flow and the wave regime, i.e., the primary bifurcation is a supercritical Hopf bifurcation. The experimental critical rotation rate (Ω_c) and critical frequency (f_c) for different stratifications are compared in Fig. 2 with theoretical values. These values come from a linear stability analysis performed with rigid boundary conditions, infinite Schmidt number, and finite gap [12].

Agreement between experiments and theory is excellent. The stabilizing effect of the stratification is demonstrated by the increase of Ω_c with the stratification.

We studied the evolution of the nondimensional frequency deviation from the critical value ($f/f_c - 1$) in the standing-wave regime (Fig. 3) as a function of the control parameter ($\epsilon = \Omega/\Omega_c - 1$) for different stratifications. All values collapse remarkably on a (-2) straight line which is predicted by a model assuming that the observed waves are internal waves confined between two vertical cylinders [12,13]. Two probes cross-correlated spectra also show that these waves are *axisymmetric*, with the phase shift for the wave frequency being equal to zero. These observations demonstrate that the system bifurcates from the purely azimuthal flow through a supercritical Hopf bifurcation to a state of axisymmetric, confined standing internal waves.

By further increasing Ω above Ω_c, a vortex regime appears. The spatiotemporal structure of this regime has also been determined with the fluorescein dye technique [Fig. 1(b)]. Overturning is depicted by the presence of the small spirals in the structures. As in the wave regime, the vertical size of the structures is compressed by the stratification, and two counterrotating vortices are present at the same height. Records of the two plane sections of the gap (not shown here) show that the flow is no longer axisymmetric. These visualizations are in good agreement with the numerical simulations of Hua *et al.* [9] and the visualizations of Boubnov *et al.* [7].

In this vortex regime, only one frequency and its harmonics are present in the power spectra. The phase shift between the two conductivity probes for the fundamental frequency is equal to the angle difference between the probes, confirming the nonaxisymmetry of the flow in this regime. We checked that the evolution of the frequency versus the rotation rate does not depend on stratification in the vortex regime (Fig. 4). The straight line fit verifies the relation $f = \alpha + m(\langle\Omega\rangle/2\pi)$, where α is a small constant, $\langle\Omega\rangle$ is the radially averaged angular velocity calculated from purely azimuthal circular Couette flow, and $m = 1$ is the azimuthal mode. In a first approximation, the whole 3D pattern is drifting at this mean angular velocity $\langle\Omega\rangle$. Because of the system's symmetries (O2), the vortices cannot drift at exactly the mean angular velocity [5]. Hence, the small value at the origin (α) is the velocity with which the pattern precesses relative to the mean angular velocity. So, the measured frequency measures the drift velocity of the pattern, i.e., the revolution period of a vortex around the axis of the cylinders.

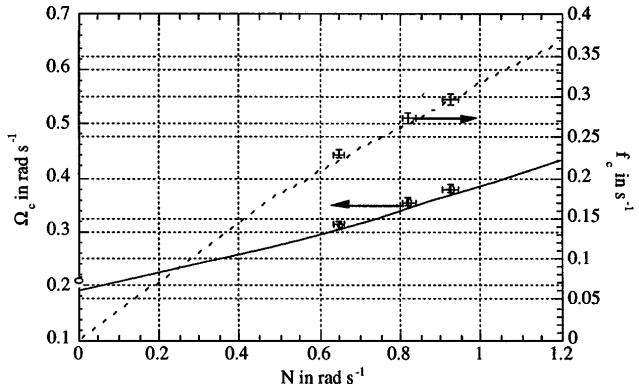

FIG. 2. Evolution of the critical rotation rate (Ω_c, left axis) and of the critical frequency of the waves (f_c, right axis) versus stratification: (○) experimental Ω_c and (solid line) theoretical curve; (+) experimental f_c and (dashed line) theoretical curve.

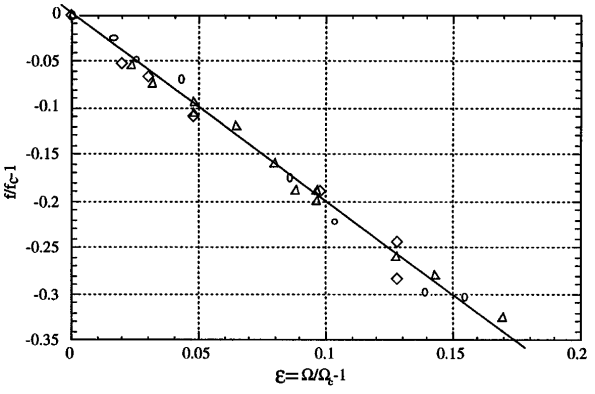

FIG. 3. Evolution of the nondimensional frequency deviation from the critical value versus ϵ in the wave regime. (◇) $N = 0.68\ \mathrm{rad\,s^{-1}}$; (○) $N = 0.82\ \mathrm{rad\,s^{-1}}$; (△) $N = 0.925\ \mathrm{rad\,s^{-1}}$. Confined internal waves model: slope (-2) straight line.

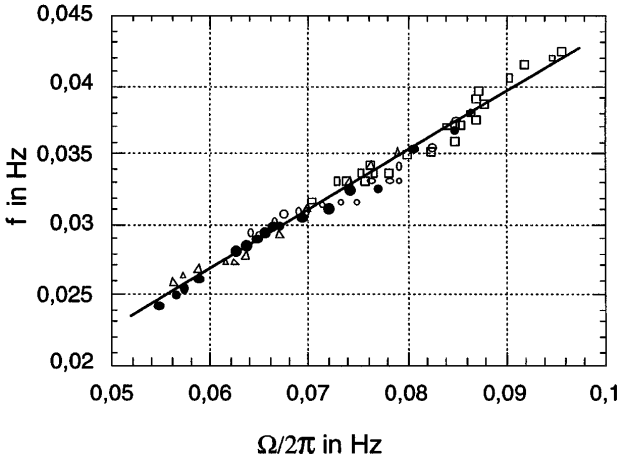

FIG. 4. Evolution of the azimuthal rotation frequency with $\Omega/2\pi$ in the vortex regime. (△) $N = 0.68\ \mathrm{rad\,s^{-1}}$; (○), (●) $N = 0.82\ \mathrm{rad\,s^{-1}}$; (□) $N = 0.925\ \mathrm{rad\,s^{-1}}$. The straight line is a linear fit: $f = 0.0027 + 0.413(\Omega/2\pi)$, $R = 0.985$.

It is determined by the cylinders geometry and the rotation rate of the inner one, so it is independent of the stratification.

Special attention has been given to the transition between the wave regime and the vortex regime. This transition does *not* correspond to the appearance or disappearance of any frequency in the spectra. The only hint of a transition is that for two probes cross-correlated spectra, the phase shift for the measured frequency is zero in the wave regime and equal to $\pi/2$ in the vortex regime. The evolution of the characteristic frequency of the power spectra versus the rotation rate when ascending or descending by small steps the control parameter is plotted on Fig. 5(a). These measurements show that the frequency can have two different values for one rotation rate, depending on the procedure. This hysteresis implies that the bifurcation between the wave regime and the vortex regime is *a subcritical bifurcation.* Moreover, the waves and vortices frequencies are equal at the transition point. Since only one frequency (corresponding to the azimuthal rotation) is present in the power spectra of the vortex regime, the limit cycle (oscillations) of the waves is destabilized in the bifurcation. From bifurcation theory, it is known that a limit cycle cannot be destabilized in a *local* bifurcation [1,3,14]. Therefore, the secondary bifurcation is a *global bifurcation.*

From these observations a plausible projection in a plane [ϵ, typical energy of mode] of the diagram of bifurcations is proposed in Fig. 5(b). The dimension of the rigorous diagram is 6: each mode energy and frequency, ϵ and N. The experimental measurement of Fig. 5(a) is its projection in a [ϵ, frequency] plane. For fixed stratification, this bifurcation diagram can be described as follows. A branch of waves is created through a direct Hopf bifurcation at the abscissa $\epsilon = 0$ (by definition). An unstable branch is created through an

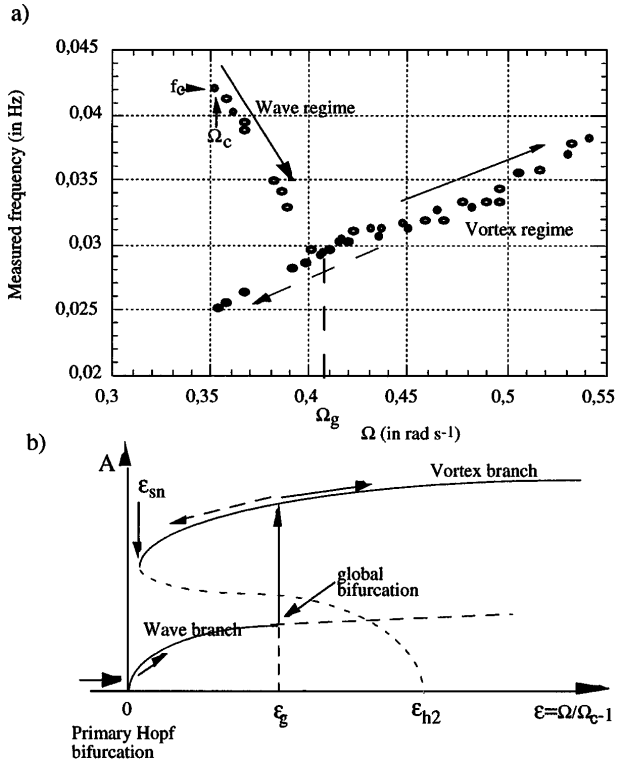

FIG. 5. (a) Hysteretic evolution of the measured frequency with the control parameter. (○) Ascending and (●) descending procedure for $N = 0.82\ \mathrm{rad\,s^{-1}}$. (b) Schematic representation of the bifurcations diagram from purely azimuthal flow to vortices. The ordinate is the energy of the perturbations to the basic state.

inverse Hopf bifurcation at the abscissa ϵ_{h2}. This unstable branch gains stability in a saddle-node bifurcation at the abscissa ϵ_{sn}, creating the branch of the vortices. At ϵ_g, the stable oscillatory branch coming from the first Hopf bifurcation is destabilized in a global bifurcation, and the system jumps onto the stable branch of the vortices. On the drifting vortices branch, if ϵ is decreased, the system will follow the vortices branch until $\epsilon = \epsilon_{\mathrm{sn}}$. Then it can jump either onto the purely azimuthal flow if $\epsilon_{\mathrm{sn}} < 0$, or onto the waves branch if $\epsilon_{\mathrm{sn}} > 0$.

From the bifurcation diagram, we are able to explain the differences between the previous results obtained with the STC system. The onset of instability in the experiments [7] is a nonaxisymmetric flow regime with vortices whereas in the direct numerical simulations [9], the onset of instability is time dependent and axisymmetric. The experimental apparatus of Boubnov *et al.* [7] had circularity defects of the order of 1 mm for a gap width of 12 mm. Such large defects induce, as we checked elsewhere [12], a sufficiently large noise amplitude to force the system to jump directly to the drifting vortices branch whenever possible. Since in these experiments, nonaxisymmetric vortices were always obtained at the onset of instability, the abscissa of the saddle-node bifurcation ϵ_{sn} was measured instead of the real onset of instability.

Comparison of these values with the theoretical critical ones shows that ϵ_{sn} is close to 0 for all the stratifications, which remains unexplained.

We provide here the first experimental evidence of the existence of such a scenario in hydrodynamics. This kind of diagram for primary and secondary bifurcations has been proposed theoretically for convection subjected to a magnetic field [11], and for binary fluid convection using numerical simulations [10,15]. Its possible existence has never been demonstrated experimentally. To our knowledge, these studies are the only ones to mention the possibility of such diagrams in hydrodynamics.

More generally, this diagram is thought to be generic for systems with two independent control parameters with opposite effects. When the typical disappearance time associated with the stabilizing control parameter is larger than the typical dissipation time of instability, the primary bifurcation is oscillatory. This is the case in several hydrodynamical systems: convection in rotating systems [5,16,17], with magnetic field [18], or in binary fluids with negative separation ratio [4,19] when, respectively, the Prandtl, magnetic Lewis, and Lewis numbers are smaller than 1. It also applies in magnetic Taylor-Couette flow [20] and obviously, in stratified Taylor-Couette when the Schmidt number is large. The case of counterrotating Taylor-Couette flow [6] is marginal since the typical times are equal.

In conclusion, we present here the first experimental evidence of a novel bifurcation diagram, for a quite simple hydrodynamical system. Indeed, the STC flow bifurcates from the purely azimuthal flow through a direct Hopf bifurcation to a wave regime. This is followed by a secondary *subcritical* Hopf bifurcation leading to a state of drifting vortices (vortex regime). From the characteristics of these two states, we propose a bifurcation diagram which reconciles the previous results obtained for the stratified Taylor-Couette system and can hold for a large class of hydrodynamical systems.

We acknowledge fruitful discussions with Bach Lien Hua, Paul Manneville, Arnaud Chiffaudel, Jean-Marc Chomaz, Jan-Bert Flor, and the technical assistance of Serge Layat. This work has been supported by CNRS (GDR-MFGA 1074).

*To whom correspondence should be addressed.
Electronic address: Beatrice.Janiaud@hmg.inpg.fr

[1] P. Manneville, *Dissipative Structures and Weak Turbulence*, Collection Aléa Saclay, Gif-sur-Yvette, France (Cambridge University Press, Cambridge, England, 1991).
[2] M. C. Cross and P. C. Hohenberg, Rev. Mod. Phys. **65**, 851 (1993).
[3] J. Guckenheimer and P. Holmes, *Non-linear Oscillations, Dynamical Systems and Bifurcations of Vector Fields* (Springer, New York, 1983).
[4] W. Schöpf and W. Zimmermann, Phys. Rev. E **47**, 1739 (1993).
[5] E. Knobloch, J. Phys. II (France) **7**, 371 (1997).
[6] C. N. Anderek, S. S. Liu, and H. L. Swinney, J. Fluid Mech. **164**, 55 (1986).
[7] B. M. Boubnov, E. B. Gledzer, and E. J. Hopfinger, J. Fluid Mech. **262**, 333 (1995).
[8] B. M. Boubnov and E. J. Hopfinger, Fluid Dyn. **32**, 520 (1997).
[9] B. L. Hua, S. Le Gentil, and P. Orlandi, Phys. Fluids A **9**, 365 (1997).
[10] E. Delouche, G. Labrosse, and E. Tric, J. Phys. III (France) **6**, 1527 (1996).
[11] A. M. Rucklidge, Nonlinearity **7**, 1565 (1994).
[12] F. Caton, Thèse de Doctorat, Université Joseph Fourier, Grenoble, 1998; F. Caton, B. Janiaud, and E. Hopfinger (to be published).
[13] D. Nicolaou, R. Liu, and T. N. Stevenson, J. Fluid Mech. **254**, 401 (1993).
[14] O. Dauchot and P. Manneville, J. Phys. II (France) **7**, 371 (1997).
[15] E. Millour, E. Delouche, E. Tric, and G. Labrosse, in *Proceedings of the Third International Meeting on Thermodiffusion* (UMH, Mons, 1998), p. 85, to be published in Entropie (1999).
[16] S. A. Thorpe, in *Notes on the 1966 Summer Study Program in Geophysical Fluid Dynamics at the Woods Hole Oceanographic Institute* (WHOI, Woods Hole, 1966), p. 80.
[17] F. Zhong, R. E. Ecke, and V. Steinberg, J. Fluid Mech. **249**, 135 (1993).
[18] S. Chandrasekhar, *Hydrodynamic and Hydromagnetic Stability* (Dover, New York, 1961).
[19] P. Kolodner, A. Passner, C. M. Surko, and R. W. Walden, Phys. Rev. Lett. **56**, 2621 (1986).
[20] T. S. Chang and W. K. Sartory, Proc. R. Soc. London A **301**, 451 (1967).